Dominant nucleon-pair configurations in low-lying states of deformed nuclei

C. Ma,[1] X. Yin,[1] and Y. M. Zhao[1,2,*]

[1]*Shanghai Key Laboratory of Particle Physics and Cosmology, School of Physics and Astronomy, Shanghai Jiao Tong University, Shanghai 200240, China*

[2]*Collaborative Innovation Center of IFSA (CICIFSA), Shanghai Jiao Tong University, Shanghai 200240, China*

(Received 8 February 2024; revised 15 March 2024; accepted 11 April 2024; published 16 May 2024)

In this paper we explicitly study dominant nucleon-pair configurations in low-lying states of deformed nuclei in two cases; the first is the schematic Elliott's SU(3) model with valence nucleons in the pf shell, and the second is the effective $V_{\text{low}-k}$ interaction with valence protons in the 50-82 shell and valence neutrons in the 82-126 shell, exemplified by ^{146}Ba and ^{148}Ce. We find that the SD nucleon-pair configurations are more predominant in low-lying states of these deformed nuclei than expected. Mixings of nucleon-pair configurations beyond the conventional SD-pair subspace, in particular, one-G and/or one-I nucleon-pair configurations, albeit small, are found to be necessary to reproduce the moment of inertia.

DOI: 10.1103/PhysRevC.109.054316

I. INTRODUCTION

The nuclear shell model (NSM) [1,2] is the most fundamental framework of low-energy nuclear structure and has been widely used in interpreting and predicting energy levels and decay modes of low-lying states [3–8]. For reviews, refer to Refs. [9–11]. However, the NSM configuration space increases explosively, and thus truncation to the configurations is indispensable. Towards this goal, collective nucleon-pair truncation, among the truncation schemes, is both very efficient and useful and has become more and more realizable. Along this line, we mention the (generalized) seniority scheme [12–16], broken pair approximation [17], the fermion dynamical symmetry model [18], and nucleon-pair approximation (NPA) [19].

In studies of the microscopic foundation of the interacting sd boson model, sd bosons are referred to as mapping images of collective SD nucleon pairs in the valence NSM configuration space [20,21]. For nearly spherical and transitional regions, there have been many discussions on validity of SD nucleon pair approximation, the studies of which demonstrate the SD-pair truncation is essentially good unless nuclei are deformed [22,23]; in other words, SD nucleon pairs are dominant in low-lying states of atomic nuclei if the deformation is not very large. Indeed, the fermion dynamical symmetry model [18]. and the SD NPA calculations [24] adopt this scenario as the configuration space to diagonalize the Hamiltonian. On the other hand, for the low-lying states of deformed nuclei, there has been a lot of discussion about the ability of the SD-pair truncation [25], and the collective nucleon pairs with higher spin (such as G pair with spin four [26]) could be essential. In recent years, numerical calculations assuming SD nucleon pairs and a few other collective nucleon pairs such as G pairs were explicitly performed in Refs. [27,28], where collective G pairs and even I pairs (with spin six) were reported to be important to reasonably reproduce the exact NSM results. However, nucleon-pair configuration space would also expand very rapidly as the number of valence nucleons increases if we consider more and more types of nucleons pairs, which renders the NPA calculations extremely complicated. So far, unfortunately, there have been few explicit studies and analyses of the roles played by collective nucleon pairs with higher spins (such as G and I) in very large nucleon-pair configurations, in low-lying states of well-deformed nuclei.

It is therefore the purpose of this paper to study the dominant configurations in low-lying states of nuclei with stable and large deformation, in particular whether or not the traditional SD nucleon pairs are dominant and whether or not collective nucleon pairs with higher spins, e.g., G and I nucleon pairs, play important roles. In this paper we focus on two cases. The first case is the Elliott's SU(3) Hamiltonian [29] in the presence of valence nucleons in the pf shell, and the second is the effective $V_{\text{low}-k}$ Hamiltonian in the presence of valence protons in the 50-82 shell and valence neutrons in the 82-126 shell. In doing so, we find that we can achieve very good approximation to the SDG or $SDGI$ configuration space by considering actually a tiny portion of the configurations beyond the collective SD nucleon-pair subspace. This means that the SD dominance in low-lying states of deformed nuclei is much more pronounced than intuitive presumptions, and more importantly, the NPA calculations yield reliable theoretical results in a very small configurations, involving of conventional SD subspace coupled with a small subspace spanned by one or two nucleon pairs other than SD pairs, which lays the foundation to simplify NPA calculations and to make the NPA much more realizable for low-lying states of well-deformed nuclei in future studies.

This paper is organized as follows. In Sec. II, we briefly introduce the NPA configuration space, and an approach of ranking basis states according to their importance to certain eigenstates, which facilitates the optimization of the model

*Corresponding author: ymzhao@sjtu.edu.cn

space with different degrees of freedom. In Sec. III and IV, the optimization of the NPA model space is discussed in the scenarios of Elliott's SU(3) model and effective $V_{\text{low}-k}$ interaction, respectively. Finally, we summarize this paper in Sec. V.

II. THEORETICAL FRAMEWORK

The NPA [19] uses collective nucleon pairs as building blocks of the configuration space. There have been constant efforts in developing the NPA for different purposes and advantages. In Ref. [30], the NPA is extended with consideration of the isospin degree of freedom; in Ref. [31], nucleon pairs with particle-hole excitations are taken into account in order to study cross-shell configurations. There have been also attempts using M-scheme bases to simplify the NPA calculations [32]. In Ref. [33], a hybrid scheme, with the M scheme in computation of matrix elements and J scheme for nucleon-pair basis states, was adopted to refine the NPA, in which the low-lying states of the well-deformed ^{152}Nd nucleus were computed in a truncated *SDGI* nucleon-pair space with effective shell-model interactions. In this section, we present a very brief introduction to the formulation of the NPA and our procedure to select the optimal nucleon-pair basis states.

A. The nucleon-pair basis state

In the NSM, a single nucleon state is denoted by quantum numbers n, l, j, and m, with n the radial number of a spherical oscillator, l the orbital angular momentum, j the total angular momentum, and m the z-axis projection, respectively. In this paper we denote a single-nucleon creation operator as $a^\dagger_j$ (i.e., nl are suppressed) to alleviate confusion. The NPA uses collective nucleon-pair basis states as building blocks of the configuration space. A collective nucleon pair with spin r and z-axis component M is defined by

$$\begin{aligned} A^{r\dagger}_m &= \sum_{j_1 j_2} y(j_1 j_2 r)\left(a^\dagger_{j_1} \times a^\dagger_{j_2}\right)^{(r)}_m \\ &= \sum_{j_1 j_2 m_1 m_2} y(j_1 j_2 r) C^{rm}_{j_1 m_1, j_2 m_2} a^\dagger_{j_1 m_1} a^\dagger_{j_2 m_2}, \end{aligned} \tag{1}$$

where j_1, j_2 run over the single-nucleon levels in the valence shell and $y(j_1 j_2 r)$ are called structure coefficients which satisfy the symmetry

$$y(j_1 j_2 r) = (-)^{j_1+j_2+r+1} y(j_2 j_1 r).$$

$C^{rm}_{j_1 m_1, j_2 m_2}$ denotes the Clebsch-Gordan coefficient. In the presence of an even number of valence nucleons, a nucleon-pair basis state is constructed by successive couplings of collective nucleon pairs, while for a system with an odd number of valence nucleons there is an unpaired nucleon coupled into the bases. The basis state with N nucleon pairs is thus defined as

$$\begin{aligned} &| \tau J_N M_N\rangle \\ &= A^{J\dagger}_M(r_0 r_1 r_2 \cdots r_N, J_1 J_2 \cdots J_N M_N) \mid 0\rangle \\ &= \{\cdots[(A^{r_0\dagger} \times A^{r_1\dagger})^{(J_1)} \times A^{r_2\dagger}]^{(J_2)} \times \cdots \times A^{r_N\dagger}\}^{(J_N)}_{M_N} \mid 0\rangle. \end{aligned} \tag{2}$$

TABLE I. Dimension of the 2^+ configuration space constructed by S, D, G, and I pairs without considering the Pauli effect. N_π and N_ν denote the numbers of proton and neutron pairs.

N_π \ N_ν	0	1	2	3	4	5	6
0	0	1	2	27	128	543	2149
1		9	71	438	2370	11187	47403
2			654	4539	26245	130060	570310
3				34127	207242	1×10^6	5×10^6
4					1×10^6	7×10^6	3×10^7
5						4×10^7	2×10^8
6							8×10^8

Here J_N and M_N are the total angular momentum of the basis state and its projection, and τ denotes additional quantum numbers of the state; $A^{r_0\dagger} = 1$ for an even system, and $A^{r_0\dagger} = a^\dagger_{j=r_0}$ for an odd system. Different from the basis states in the NSM, the NPA configuration basis states are in principle not orthogonal with each other. This feature leads to additional complexity in selecting important configurations in the model space, as we shall see in next subsection.

In this paper, the collective nucleon pairs, both the spin-parity and their structure coefficients, are obtained by projecting unconstrained Hartree-Fock (HF) ground state with consistent interactions [27]. This method provides us with a good estimation for the importance of each pair and has been used widely for deformed nuclei [27,28,34–36]. In all cases of this paper we find that the most important S, D, G, and I pairs constitute over 95% of the HF ground state. We thus use the *SDGI*-pair approximation and take these four pairs to construct the configuration space.

For nuclei with both valence protons and neutrons, the model space is constructed by coupling the nucleon-pair basis states of valence protons and those of valence neutrons, denoted by $(|\pi\tau J\rangle \times |\nu\tau' J'\rangle)^{(I)}$, where π and ν represent proton and neutron systems, respectively. We note that such nucleon-pair configuration space becomes very large with the number of proton and neutron pairs increased. Table I presents the dimensions of 2^+ spaces constructed by the above pairs without considering the Pauli effect. In previous papers it was required that the number of non-S pairs in the model space be small, particularly, and with few exceptions, the number of pairs beyond *SD* nucleon pairs was very small (one or two) in NPA calculations. In this paper, we shall investigate whether this simplification is warranted, and furthermore, we wish to determint the *minimal and optimal* configurations involving G and I nucleon pairs.

To facilitate our discussion, in this paper we shall call the configuration space constructed by using *SDGI* nucleon-pair basis, with the number of all these four types of pairs from zero to the total pair number (which is three or four in this paper), as the full *SDGI* nucleon-pair configuration space, despite that it is one subspace and is much smaller than the exact shell-model configuration space, as it is generally believed that this *SDGI* nucleon-pair configuration space is a very good approximation of the exact shell model space even for very large shells and for deformed nuclei. Furthermore, we shall

also investigate some smaller configuration spaces obtained by limiting the numbers of G and/or I pair. For convenience, we denote these spaces by *SDmGnI* with m and n the maximal numbers of G and I pairs in the NPA basis states.

B. Procedure to optimize nucleon-pair basis states

In previous studies [37–41], the overlap between two normalized states was usually used to evaluate the validity of an approximate wave function for given eigenstate Ψ of the system. If $\{\varphi_i\}$ is a set of orthogonal bases, then Ψ can be expanded in terms of φ_i, that is, $\Psi = \sum_i \alpha_i \varphi_i$ with $\sum_i |\alpha_i|^2 = 1$. If $|\langle\varphi_i|\Psi\rangle|^2 = |\alpha_i|^2$ is close to 1, then one could say that φ_i is a very good approximation to Ψ. In realistic practice, among all basis states φ_i, one selects the basis state with the largest magnitude of α_i as the optimized approximate wave function; if $|\alpha_i|$ is not large enough, then one further includes the next basis state $\varphi_{i'}$ with the second-largest magnitude of $\alpha_{i'}$, and the configuration space becomes two dimensional. This process continues until the sum of $|\alpha_i|^2 + |\alpha_{i'}|^2 + \cdots$ is close to 1. This is a common practice in computation in quantum mechanics.

However, this practice is not straightforward for (normalized) nonorthogonal basis states. Suppose that two basis vectors, φ_i and $\varphi_{i'}$, are nearly parallel and the overlaps $\langle\varphi_i|\Psi\rangle \simeq \langle\varphi_{i'}|\Psi\rangle$. In optimizing the basis states, one keeps only one of them. A simple way to avoid this issue is to incorporate the Schimidt orthogonalization in the selection process. Below we describe our procedure of optimizing nucleon-pair basis from the full *SDGI* configuration space.

Our NPA wave function $|\Psi_\alpha\rangle$ in the full *SDGI* nucleon-pair space is expanded as follows:

$$|\Psi_\alpha\rangle = \sum_{iJ,i'J'} \Psi^{(\alpha)}_{iJ,i'J'} \left[\left|\psi^{(J)}_{\pi i}\right\rangle \times \left|\psi^{(J')}_{\nu i'}\right\rangle \right]^{(I_\alpha)}, \tag{3}$$

where $|\psi^{(J)}_{\eta i}\rangle$ represents a complete set of normalized proton ($\eta = \pi$) or neutron ($\eta = \nu$) nucleon-pair basis states, with J being the spin quantum number and i the additional quantum number. α is the label of the eigenstate in the *SDGI* nucleon-pair configuration space. Here squared overlap explicitly reflects whether a basis state is a dominant component of $|\Psi_\alpha\rangle$.

In our procedure of optimizing the basis states for valence protons, the first nucleon-pair basis state we select, $|\pi\sigma_1 J_1\rangle$, has the largest squared overlaps with $|\Psi_\alpha\rangle$, defined by

$$\begin{aligned} P^{(\alpha)}_{\pi\sigma J} &\equiv \sum_{i'J'} |\langle \pi\sigma J, \nu i'J'; I_\alpha|\Psi_\alpha\rangle|^2 \\ &= \sum_{ii'J'} \left|\langle \pi\sigma J|\pi i J\rangle \Psi^{(\alpha)}_{iJ,i'J'}\right|^2. \end{aligned} \tag{4}$$

Then, before we obtain next proton basis state, the Schimidt orthogonalization is performed. The residual basis states are transformed to

$$\left|\varphi^{(2,J)}_{\pi\sigma}\right\rangle = \mathcal{N}(1 - |\pi\sigma_1 J_1\rangle\langle\pi\sigma_1 J_1|)|\pi\sigma J\rangle,$$

with $\mathcal{N}$ the normalization factor. Now we search for the second optimal basis state by calculating squared overlap $P^{(\alpha)}_{\pi\sigma J}$ defined in Eq. (4), except that $|\pi\sigma J\rangle$ should be replaced by using $|\varphi^{(2)}_{\pi\sigma J}\rangle$, and obtain the second-most-optimal basis state $|\pi\sigma_1 J_1\rangle$. In general we define

$$\begin{aligned} \left|\varphi^{(k,J)}_{\pi\sigma}\right\rangle &= \mathcal{N}\left[1 - \sum_{a=1}^{k-1} \left|\varphi^{(J_a)}_{\pi\sigma_a}\right\rangle\left\langle\varphi^{(J_a)}_{\pi\sigma_a}\right|\right]|\pi\sigma J\rangle \\ &= \mathcal{N}\left[1 - \left|\varphi^{(J_{k-1})}_{\pi\sigma_{k-1}}\right\rangle\left\langle\varphi^{(J_{k-1})}_{\pi\sigma_{k-1}}\right|\right]\left|\varphi^{(k-1)}_{\pi\sigma J}\right\rangle, \end{aligned} \tag{5}$$

$$P^{(k,\alpha)}_{\pi\sigma J} = \sum_{ii'J'} \left|\left\langle\varphi^{(k,J)}_{\pi\sigma}\middle|\psi^{(J)}_{\pi i}\right\rangle \Psi^{(\alpha)}_{iJ,i'J'}\right|^2, \tag{6}$$

where $|\varphi^{(J_k)}_{\pi\sigma_k}\rangle$ is the orthogonalized state $|\varphi^{(k,J)}_{\pi\sigma}\rangle$ with its squared overlaps $P^{(\alpha)}_{\pi\sigma_k J_k}$ being the largest one over $P^{(k,\alpha)}_{\pi\sigma J}$. This procedure is iterated until one achieves satisfactorily $\sum_k P^{(\alpha)}_{\pi\sigma_k J_k}$ which is very close to 1.

Similarly, one optimizes the nucleon-pair basis states for valence neutrons.

Following the above procedure, we can conveniently discuss the effect of truncation to the model space by different degrees of freedom according to the optimal order for proton (neutron) basis states.

III. SCHEMATIC ELLIOTT'S SU(3) MODEL

In this section, we study the pf shell with isospin-conserved quadrupole-quadrupole interaction,

$$\begin{aligned} V_Q &= -(Q_\pi + Q_\nu)\cdot(Q_\pi + Q_\nu) \\ &= -\sqrt{5}[(Q_\pi + Q_\nu)\times(Q_\pi + Q_\nu)]^{(0)}, \end{aligned} \tag{7}$$

with Q_π and Q_ν the quadrupole spherical harmonics of protons and neutrons in terms of both the coordinate $\vec{r}$ and the momentum $\vec{p}$,

$$Q = \tfrac{1}{2}\left[r^2 Y^{(2)}(\Omega_r) + r_0^4 \hbar^{-2} p^2 Y^{(2)}(\Omega_p)\right], \tag{8}$$

where the magnetic quantum number has been omitted without confusion and $r_0^2 = 1.012A^{1/3}$ fm^2. Ω_r and Ω_p are the polar angles of $\vec{r}$ and $\vec{p}$, respectively. It is easy to prove that Q conserves the principal quantum number of the oscillator basis and thus has a closed second quantization form in one major shell,

$$Q = \sum_{j_1 j_2} q(j_1 j_2)\left(a^\dagger_{j_1} \times \tilde{a}_{j_2}\right)^{(2)}, \tag{9}$$

with j_1, j_2 running over the single-nucleon levels in the major shell. The coefficients $q(j_1 j_2) = \frac{(-)^{j_1+1/2}}{\sqrt{20\pi}}\sqrt{2j_1+1}\ \sqrt{2j_2+1}C^{20}_{j_1 1/2, j_2 -1/2}\langle n_1 l_1|r^2|n_2 l_2\rangle$, where $C^{20}_{j_1 1/2, j_2 -1/2}$ is the Clebsch-Gordan coefficient. Equation (9) is used to construct V_Q in our NPA calculations.

This interaction is very interesting, because one is able to obtain the exact and analytical shell-model results with the help of the Elliott model [29], regardless of how enormous the shell-model space might be. The interaction in Eq. (7) respects the SU(3) symmetry of the Elliott model, according to which the eigenvalue is given in terms of the irreducible representation quantum numbers of SU(3) group, (λ, μ), and irreducible representation quantum number of the SO(3) group, L, by

$$E = -\frac{5}{2\pi}\left[\frac{1}{2}(\lambda^2 + \lambda\mu + \mu^2 + 3\lambda + 3\mu) - \frac{3}{8}L(L+1)\right]. \tag{10}$$

For $\mu = 0$, the reduced electric quadrupole transition probability is given by

$$B(E2; L \to L') = \frac{5e_{\rm eff}^2}{16\pi}\frac{(2L+1)}{(2L'+1)}\left[\frac{c_{L'}}{c_L}C^{L'0}_{L0,20}\right]^2 \times \left[2\lambda + 3 + \frac{1}{2}L'(L'+1) - \frac{1}{2}L(L+1)\right]^2, \tag{11}$$

where $e_{\rm eff}$ is the effective charge for both protons and neutrons, $C^{L'0}_{L0,20}$ the Clebsch-Gordan coefficient, and

$$c_L = \left[\frac{(2L+1)2^L\lambda!(\frac{1}{2}\lambda+\frac{1}{2}L)!}{(\lambda+L+1)!(\frac{1}{2}\lambda-\frac{1}{2}L)!}\right]^{\frac{1}{2}}.$$

For $\mu \neq 0$, however, there is no available formula to obtain exact $B(E2)$ value. Instead, one can derive an approximate value by neglecting the nonorthogonality of eigenstates from intrinsic states with different projection. From the Eq. (45) of Ref. [29], we get an approximate expression,

$$B(E2; L \to L') = \frac{5e_{\rm eff}^2}{16\pi}\frac{(2L+1)}{(2L'+1)}\left[\frac{\tilde{c}_{L'}}{\tilde{c}_L}C^{L'0}_{L0,20}\right]^2 \times \left[2\lambda + \mu + 3 + \frac{1}{2}L'(L'+1) - \frac{1}{2}L(L+1)\right]^2, \tag{12}$$

which differs from Eq. (11) mainly in terms of the coefficient $\tilde{c}_L$ obtained through an iterative technique. This approximation is good for the states with low angular momenta. Several useful SU(3) representations for low-lying states can be found in Refs. [42–44]. It is also worth noting that an additional single-particle term is necessary in order to reproduce the above results in the shell-model calculation if the momentum-dependent part in Eq. (8) is omitted [45].

Now we come to a system of six protons and six neutrons in the pf shell in the presence of interaction defined in Eq. (7). Figure 1 shows the excitation energies and $B(E2)$ of the ground band states calculated in nucleon-pair subspaces as well as corresponding results given by Eqs. (10) and (11) with $(\lambda, \mu) = (24, 0)$ of the Elliott model, namely the exact NSM results. The effective charge $e_{\rm eff} = 1.0e$ for sake of simplicity. We find that the NPA calculation in the full *SDGI*-pair space exactly reproduces all excitation energies and $B(E2)$ for the ground band; on the other hand, NPA calculations in the *SD*- and *SDG*-pair subspaces yield only 38.7% and 58.5% of the exact moment of inertia and much smaller $B(E2)$ values. However, one should be careful in comments of the *SD*- or *SDG*-pair approximations, as the structure coefficients here are obtained using the Hartree-Fock approach [27,28]. It has been reported in Ref. [35] that the *SDG*-pair space with the structure coefficients of *S*, *D*, and *G* pairs optimized using the conjugate gradient (abbreviated as CG in this paper) approach is sufficient to exactly reproduce these ground band states. The disadvantage to obtain the nucleon-pair structure coefficients by the CG approach is that this approach requires repetitions of NPA calculation for hundreds or even thousands of times, and this makes the application of CG approach much less practical for realistic nuclei with stable deformation.

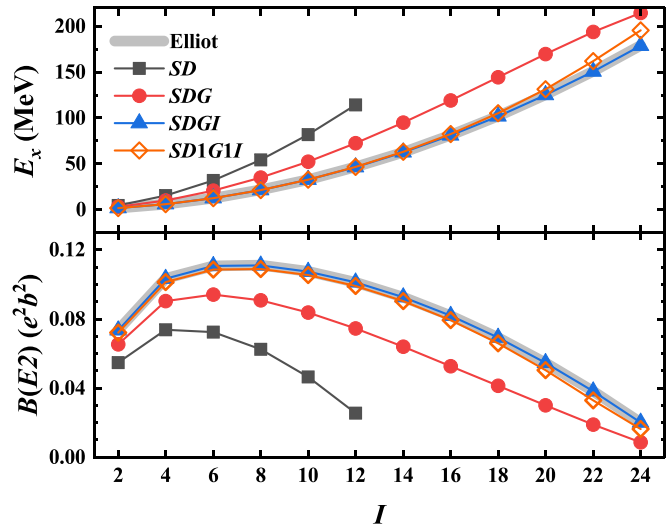

FIG. 1. Excitation energy $E_x(I)$ and reduced electric transition probability $B(E2; I \to I-2)$ for the ground band states of six valence protons and six valence neutrons in the pf shell versus spin I of the states. "Elliott" denotes the results based on the Elliott's SU(3) model. "*SD*," "*SDG*," and "*SDGI*" denote configurations constructed by collective *SD*, *SDG*, and *SDGI* nucleon pairs, respectively. "*SD*1*G*1*I*" denotes *SD* nucleon pair subspace coupled to a space with one *G* and/or one *I* pair (in addition to *SD* nucleon pairs).

It is very interesting, as shown in Fig. 1, that the *SDGI*-pair approximation with the requirement of *G* and *I* pair number equal to or below 1, denoted by "*SD*1*G*1*I*," also reproduces the excitation energies and the $B(E2)$ values very well, except for states with spins close to maximum. The dimension of this "*SD*1*G*1*I*" subspace is only about a fifth of the full *SDGI*-pair space. This means most of the *SDGI*-pair configurations with *G* pair number more than 1 do not play any essential roles, at least for the ground band structure.

Therefore it is informative to investigate, among the full *SDGI* pair configurations, those basis states which play important roles in low-lying states. Towards this goal, we make use of the procedure to optimize the nucleon-pair basis, discussed in Sec. II B. We first obtain the wave functions of states in the full *SDGI*-pair space and calculate the squared overlap $P^{(\alpha)}_{\eta\sigma_k J_k}$ for each proton (or neutron) basis state. In Fig. 2 we show the sum of these squared overlaps of a given nucleon-pair configuration for the low-lying 0^+_1, 2^+_1, 4^+_1, and 6^+_1 states. One finds that the pattern of $P^{(\alpha)}_{\eta\sigma_k J_k}$ in terms of various nucleon-pair configurations are very similar to each other for different eigenstates. This is clearly distinct from the cases in spherical and vibrational nuclei, where the "nucleon-pair states" dominating in the eigenstates can be drastically different [41]. Another important feature exhibited in Fig. 2 is that the dominant configurations of these low-lying states of the ground rotational band are constructed by *S* and *D* nucleon pairs, and the most important configurations are given by D^3 and SD^2; these configurations together with *SSD* and *SSS* account for *more than 50%* in wave functions of those states. Furthermore, we also see that the *SD* nucleon-pair

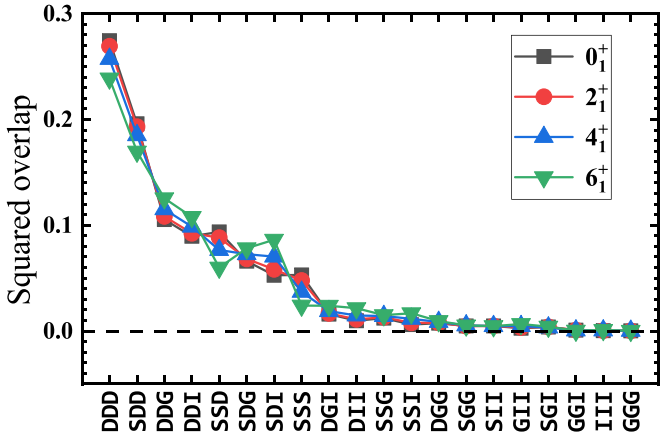

FIG. 2. Squared overlaps, $\sum_{\sigma_k J_k} P^{(\alpha)}_{\eta\sigma_k J_k}$ [see Eq. (4), where $\eta = \pi$ (or ν), σ specifies a nucleon-pair subspace, and α denotes an eigenstate], with the wave functions calculated in the full *SDGI* pair configuration space. The results in black, red, blue, and green correspond to 0_1^+, 2_1^+, 4_1^+, and 6_1^+ states, respectively.

subspace, generalized by considering more one-G and/or -I nucleon pairs, denoted by $SD1G1I$ nucleon-pair space, very well overlap with the full *SDGI* configuration space. The squared overlap of the top nine configurations of the $SD1G1I$ space in the 0_1^+, 2_1^+, 4_1^+, and 6_1^+ states is 0.95, 0.94, 0.93, and 0.92, respectively.

The result, that the very large *SDGI* nucleon-pair space is well represented by its $SD1G1I$ subspace, is very encouraging. For $N_\pi = N_\nu = 3$ in the $SD1G1I$ nucleon-pair subspace, the numbers of 0^+, 2^+, 4^+, and 6^+ states are 1146, 5211, 8014, and 9047, respectively. One would ask whether this subspace can be further reduced without expensive cost of accuracy for calculated results. Figure 3 presents the calculated excitation energies and the $B(E2)$ values of the 2_1^+, 4_1^+, and 6_1^+ states in truncated model spaces spanned by proton and neutron pair basis states, $|\eta\sigma_k J_k\rangle$ with $k = 1 \sim N_{\rm ps}$, with the optimal procedure of Sec. II B. As shown in Fig. 3, we obtain good agreement with calculated results of the full *SDGI* space at $N_{\rm ps} = 50$, for which the dimensions of the 0^+, 2^+, 4^+, and 6^+ spaces are only 518, 1405, 1929, and 2005, respectively.

Figures 4–6 present similar investigations but for eight valence protons and eight valence neutrons in the pf shell. In Fig. 4 the Elliott's excitation energies and $B(E2)$ values are given by Eqs. (10) and (12) with $(\lambda, \mu) = (20, 8)$, respectively. We note that Eq. (12) is close to the exact NSM value in the limit of very low spins (I is small), as the value of $\mu \neq 0$ in this case. From Figs. 4–6, we see that the *SDG*-, *SDGI*-, as well as $SD1G1I$-pair approximations are in good agreement for excitation energies and exhibit discernible but very small differences for $B(E2)$ values, in comparison with the results of Eqs. (10) and (12); and the agreement between these NPA results, in particular, the *SDGI* NPA, and those of the Elliott model, are very good. The difference of NPA calculated $B(E2)$ values between the *SDGI* and the $SD1G1I$ results means that the transition probability is much more sensitive to the details of wave functions than eigenenergies. Indeed, as shown in Fig. 5, configurations with two I nucleon pairs also

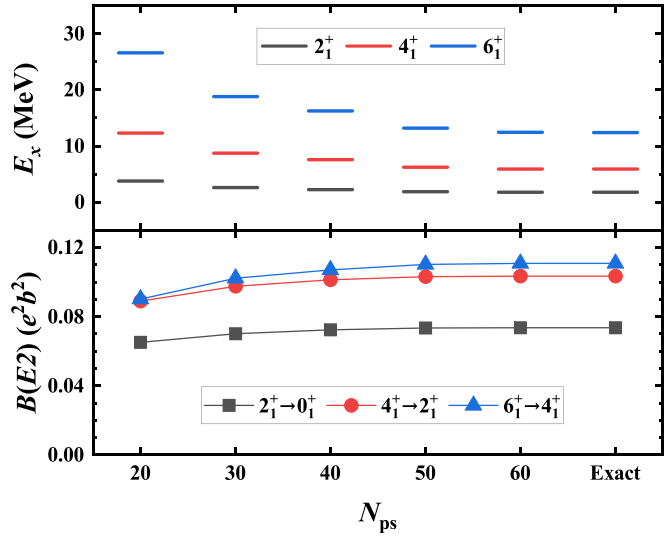

FIG. 3. Excitation energy and reduced electric transition probability for the 2_1^+, 4_1^+, and 6_1^+ states versus the number of selected optimal neutron-pair basis states for systems of $N_\pi = N_\nu = 3$ in the presence of the Hamiltonian of Eq. (7) and in the pf shell. The exact results are derived from the Elliott's SU(3) model according to Eqs. (10) and (11).

contribute considerably large to the ground rotational bands of this system. Actually, the $SD1G2I$-pair approximation does reproduce the $B(E2)$ values given by the calculation in the full *SDGI* model space. Similarly to our above study of the $N_\pi = N_\nu = 3$ case, we find that we achieve very good results at $N_{\rm ps} = 500$, as shown in Fig. 6.

IV. ^{146}Ba AND ^{148}Ce WITH EFFECTIVE INTERACTION $V_{{\rm low}-k}$

With the same motivation as in Sec. III, here we investigate the optimal nucleon-pair basis states of low-lying

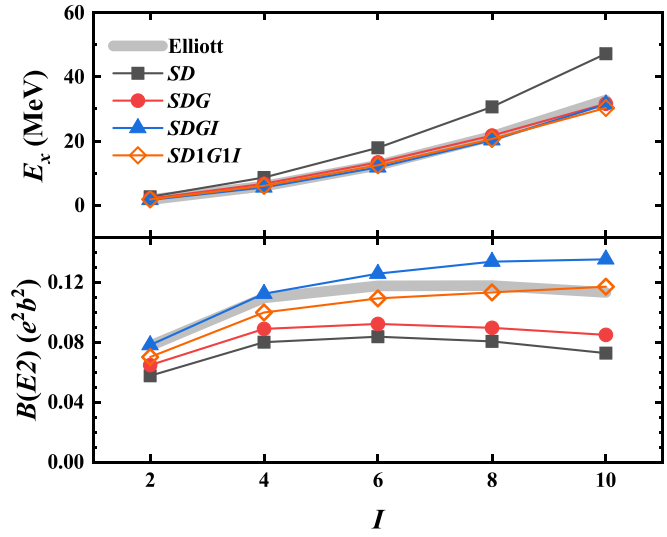

FIG. 4. Same as Fig. 1 but for the system with eight valence protons and eight valence neutrons in the pf shell.

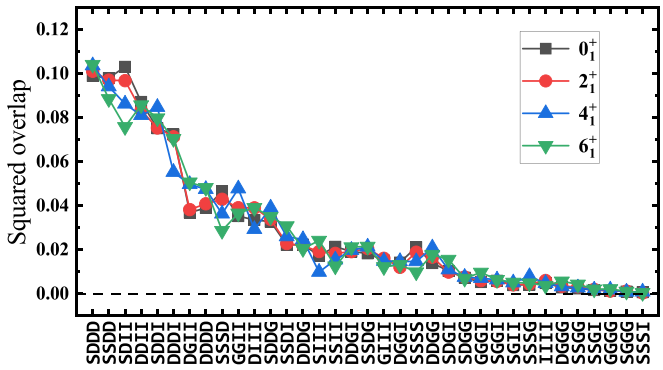

FIG. 5. Same as Fig. 2 but for the system with eight valence protons and eight valence neutrons in the pf shell.

states, exemplified by two realistic nuclei, ^{146}Ba and ^{148}Ce, in the presence of effective interactions. For both nuclei, we use ^{132}Sn as the inert core and take the experimental spectra of ^{133}Sb and ^{133}Sn [46] as the single-particle energies of the Hamiltonian, as shown in Table II. The two-body effective matrix elements are obtained by integrating the model-independent low-momentum nucleon-nucleon interaction [47,48], known as $V_{\text{low}-k}$, sandwiched between the harmonic oscillator wave functions with the oscillator parameter $\hbar\omega = 7.87$ MeV. The effective charges are taken as $e_\pi = 2.0\,e$ and $e_\nu = 1.0\,e$ for the $B(E2)$ evaluation; the effective factors $g_{l\pi} = 1.0\,\mu_N$, $g_{l\nu} = 0$, $g_{s\pi} = 5.586\times 0.7\,\mu_N$, and $g_{s\nu} = -3.826\times 0.7\,\mu_N$ are taken for the calculation of magnetic dipole moments μ.

Figure 7 plots the NPA-calculated excited energies of ground band states in the *SDG*, *SD*1*G*1*I*, and the full *SDGI* nucleon-pair spaces in comparison with corresponding experimental data taken from Ref. [46]. One sees that all these calculations predict the quasirotor structure, while the inertia moments of the *SDG* and *SD*1*G*1*I* nucleon-pair approximations are smaller than the result of the *SDGI* approximation:

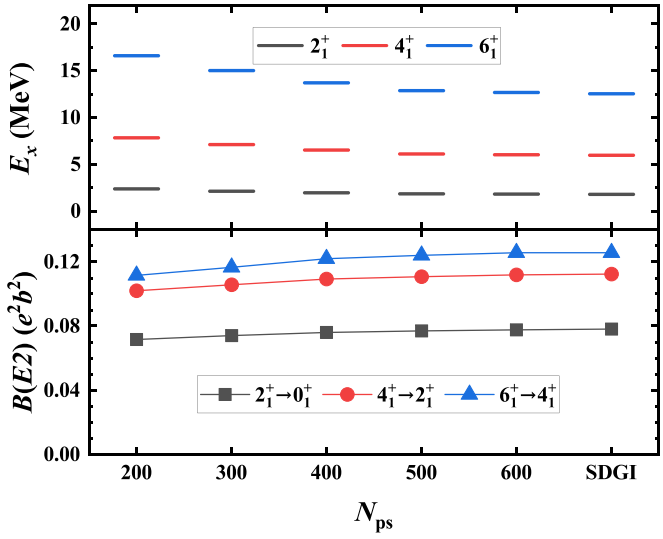

FIG. 6. Same as Fig. 3, but for the system with eight valence protons and eight valence neutrons in the pf shell.

TABLE II. Single-particle energies of valence protons (π) and valence neutrons (ν) taken from the experimental spectra of ^{133}Sb and ^{133}Sn [46].

j_π	$2s_{1/2}$	$1d_{3/2}$	$1d_{5/2}$	$0g_{7/2}$	$0h_{11/2}$	
ϵ_{j_π}	2.990	2.440	0.962	0.000	2.793	
j_ν	$2p_{1/2}$	$2p_{3/2}$	$1f_{5/2}$	$1f_{7/2}$	$0h_{9/2}$	$0i_{13/2}$
ϵ_{j_ν}	1.363	0.854	2.005	0.000	1.561	2.690

23.7(7), 27.9(7), and 35.3(6) $\hbar^2\text{MeV}^{-1}$ for ^{146}Ba, and 22.9(5), 28.4(6), and 33.3(6) $\hbar^2\text{MeV}^{-1}$ for ^{148}Ce, given respectively by linear fitting to the 2_1^+, 4_1^+, and 6_1^+ states in the three model spaces. This indicates that some configurations out of the *SD*1*G*1*I* space also come into play, although their contribution to the wave functions may be very small [49].

Next we investigate the electromagnetic properties of our calculations. Tables III and IV present the $B(E2)$ and g values of low-lying yrast states calculated by the *SDG*, *SD*1*G*1*I*, and *SDGI* approximations. We also compare these values to experimental data from the NNDC and the theoretical results from the rotational model (RM), given by

$$B(E2; IK) = \frac{5}{16\pi}\left(C^{I\text{-}2\,K}_{IK,20}Q_0\right)^2,$$

$$g = Z/A,$$

where the magnetic quantum number in the intrinsic space $K = 0$ and the intrinsic quadrupole moment is regarded as a parameter and taken $Q_0 = 5.0$ eb; Z and A are the proton number and the mass number, respectively. In the aspect of the $B(E2)$ values, there are no significant differences among the three sets of the NPA calculations. Also our calculations are close to the experimental data and the RM results. On the other hand, the gyromagnetic ratios obtained from the NPA calculations are systematically larger than the experimental and the RM values, especially for ^{146}Ba. One possible reason for this difference is that the magnetic moment is sensitive to the nuclear wave functions and thus magnifies the impact of nucleon-pair truncation. As manifested by our calculations,

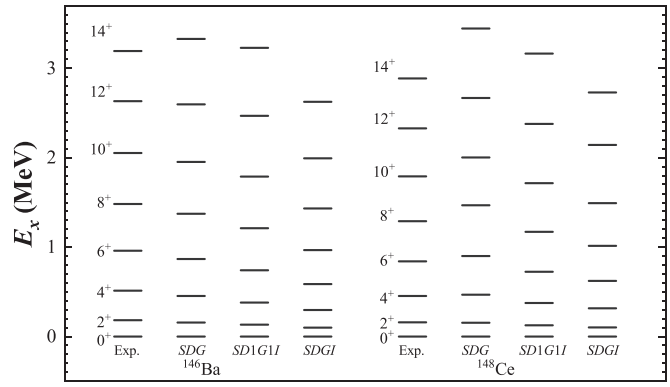

FIG. 7. Excitation energies of the yrast states for ^{146}Ba and ^{148}Ce. Experimental data are taken from the NNDC [46] database, and "*SD*," "*SDG*," "*SD*1*G*1*I*," and "*SDGI*" correspond to calculated results in *SD*, *SDG*, *SD*1*G*1*I*, and *SDGI* nucleon-pair configuration spaces.

TABLE III. Electric quandrupole transition probability $B(E2)$ (in e^2b^2) for low-lying states of ^{144}Ba and ^{148}Ce. Experimental data are taken from the NNDC [46] database. Calculated results are obtained in the *SD*, *SDG*, *SD*1*G*1*I*, and *SDGI* nucleon-pair configuration spaces. Our effective charges $e_\pi = 2.0\,e, e_\nu = 1.0\,e$. The corresponding results of the rotational model (RM) are also calculated by assuming $K = 0$ and the intrinsic quadrupole moment $Q_0 = 5.0\,e$b.

Nuclide	State	Expt.	*SDG*	*SD*1*G*1*I*	*SDGI*	RM
^{146}Ba	2_1^+	0.27(1)	0.45	0.45	0.49	0.50
	4_1^+	0.73(64)	0.65	0.65	0.71	0.71
	6_1^+		0.70	0.71	0.77	0.78
	8_1^+		0.71	0.72	0.78	0.82
^{148}Ce	2_1^+	0.40(3)	0.47	0.48	0.50	0.50
	4_1^+	>0.02	0.68	0.69	0.72	0.71
	6_1^+		0.73	0.74	0.78	0.78
	8_1^+		0.72	0.75	0.79	0.82

the *g* factors obtained from the full *SDGI*-pair space are closer to the experimental value than those from the truncated *SDG*- and *SD*1*G*1*I*-pair spaces. The deviation of the RM result from the experimental value is also sizable, indicating that ^{146}Ba is not a perfect rotating rigid nucleus.

In order to understand the differences of calculated $B(E2)$ and μ in those nucleon-pair spaces, we investigate squared overlaps between the low-lying states in the *SDGI* nucleon-pair space and each proton-neutron basis states, with the iteration procedure introduced in Sec. II B concerning the nonorthogonal issue. We note that overlaps belonging to same proton-neutron configuration are integrated. In Fig. 8, we plot the contributions of various nucleon-pair configurations to the yrast 0_1^+ and 2_1^+ states of the ^{148}Ce nucleus, where one sees clearly that *SD* nucleon-pair contribution are by far predominant in these states, with slight mixings of the one-*G*-pair and/or one-*I*-pair and two-*G*-pair configurations; contribution from other nucleon-pair configurations are tiny and negligible in these states. In quantitative terms, the pure *SD*-pair configurations account for 55% and 47% of the wave functions for the 0_1^+ and 2_1^+ states, while the squared overlaps increase to over 90% if we take the mixings of one-*G* and/or -*I* pair into account.

TABLE IV. Same as in Table III but for gyromagnetic ratio *g* (in $\mu_N/\hbar$). The effective parameters are taken $g_{l\pi} = 1.0\,\mu_N$, $g_{l\nu} = 0$, $g_{s\pi} = 5.586\times0.7\,\mu_N$, and $g_{s\nu} = -3.826\times0.7\,\mu_N$. The rotational model (RM) predicts $g = Z/A = 0.38$ and 0.39 for ^{146}Ba and ^{148}Ce, respectively.

Nuclide	State	Expt.	*SDG*	*SD*1*G*1*I*	*SDGI*
^{146}Ba	2_1^+	0.26(5)	0.52	0.53	0.47
	4_1^+		0.54	0.55	0.49
	6_1^+		0.56	0.57	0.50
	8_1^+		0.59	0.58	0.52
^{148}Ce	2_1^+	0.38(5)	0.47	0.42	0.41
	4_1^+		0.51	0.45	0.42
	6_1^+		0.55	0.47	0.43
	8_1^+		0.62	0.48	0.44

In Fig. 9 we present the marginal distribution of squared overlaps in each proton- and neutron-pair configuration for the yrast 0^+, 2^+, 4^+, and 6^+ states of ^{146}Ba and ^{148}Ce. One sees that, as in the two cases in last section for the Elliott model, the differences of contributions from each proton and neutron nucleon-pair configuration is quite small for different states in the yrast band (except for the *S*-pair condensate configuration and the one-broken-pair *SD* configuration). This indicates the "robustness" of the contribution of pair configurations to different low-lying states in the deformed nuclei.

On the other hand, proton and neutron nucleon-pair configurations exhibit different behaviors. This is understandable, because valence protons and neutrons are in different shells in the presence of different interactions. For valence protons, configurations including one *I* pair are of importance to reproduce the wave functions of low-lying states; the *DDI*, *SDI*, *DGI*, and *SGI* configurations in the proton system of ^{146}Ba also contribute considerable overlaps, and this pattern survives for ^{148}Ce. This is why the *SDG*-pair approximation deviates from the full *SDGI* nucleon-pair approximation. As for the neutron part of the low-lying states of ^{146}Ba and ^{148}Ce, the contribution from the *SDDG*, *SSDG*, *DDDG*, and *SDGG* pair configurations are not negligible, and the two-*G*-pair configuration (i.e., *SDGG*) is the reason the *SD*1*G*1*I*-pair approximation presents slight deviations in comparison with the full *SDGI* nucleon-pair space. To demonstrate this is indeed the case, we present the calculated results in the subspace constructed by the proton *SD*1*G*1*I*-pair and the neutron *SD*2*G*1*I*-pair configurations, which reproduce very well the results of the *SDGI* approximation; e.g., calculated energies of the 2_1^+, 4_1^+, and 6_1^+ states of ^{146}Ba are 0.10, 0.31 and 0.63 MeV in this subspace, while the corresponding results are 0.10, 0.30, and 0.59 MeV in the full *SDGI* nucleon-pair configuration. Those for for ^{148}Ce are 0.11, 0.33, and 0.65 MeV in this subspace while the corresponding results are 0.10, 0.32, and 0.62 MeV in the *SDGI* nucleon-pair space.

It is also very interesting to point out once again that for low-lying states of these two nuclei, the first two configurations are *SDD* and *SSD* for the proton part of ^{146}Ba and *SSDD*, *SSSD* for the neutron part of ^{146}Ba and both parts of ^{148}Ce, with their squared overlaps significantly larger than other configurations. Moreover, the integrated overlaps of the *SD*-pair configurations for the low-lying states of these two nuclei (except the 6_1^+ state of ^{146}Ba) are *over 50%*, as shown in Table V. These integrated overlaps of *SD* nucleon-pair subspace for realistic nuclei using the shell-model effective interaction are even larger than those obtained from the Elliott SU(3) model. It thus provides us with evidence of the *SD*-pair dominance in the low-lying states of realistic deformed nuclei.

It is noteworthy that, on the one hand, the *SD*1*G*1*I*-pair subspace yields calculated results with slight deviations in comparison with calculated results in the full *SDGI* configuration space, as shown in Tables III and IV and Fig. 7, and, on the other hand, Fig. 9 demonstrates that the *SD*1*G*1*I*-pair subspace contributes essential components of the full *SDGI* configuration; all integrated squared overlaps of the *SD*1*G*1*I* configurations are *larger than 0.91*. This means that calculated

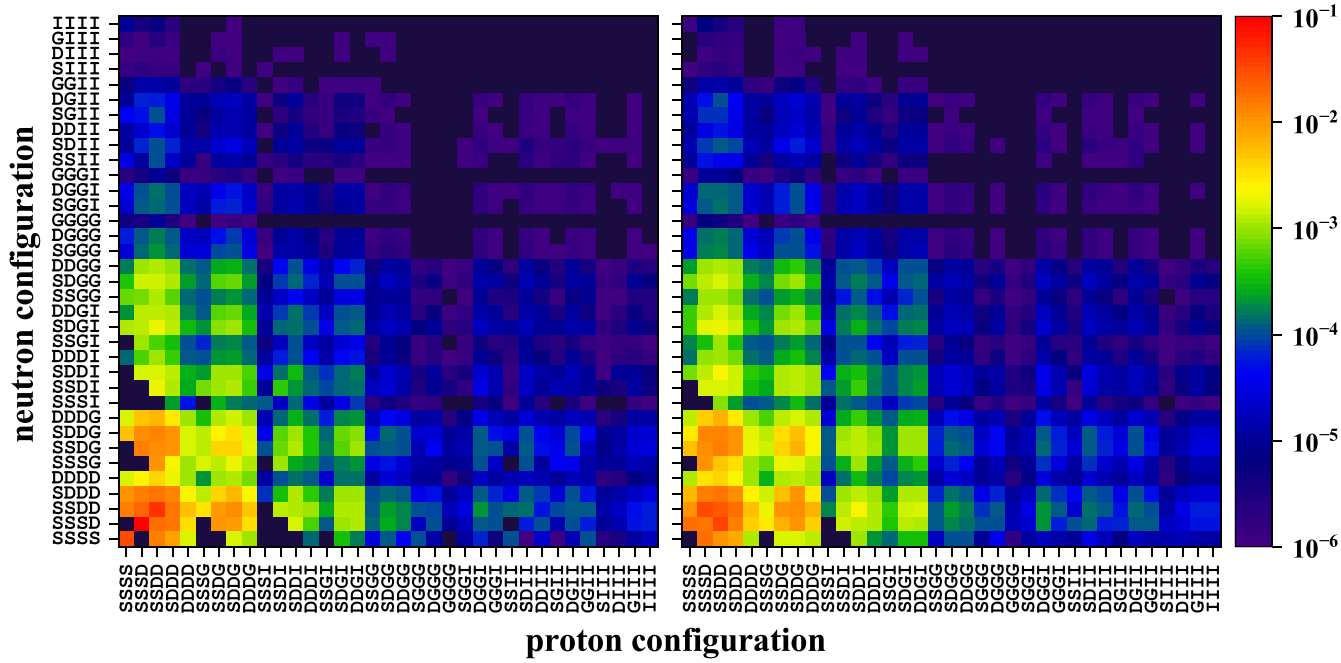

FIG. 8. Contribution from various nucleon-pair configurations in the yrast 0_1^+ and 2_1^+ states of the ^{148}Ce nucleus, in wave functions calculated by using the full *SDGI* nucleon-pair configuration space. Calculation of squared overlaps are performed via the procedure of Sec. II B in this paper. Left panel corresponds to the 0_1^+ state, and the right panel corresponds to the 2_1^+ state. The results plotted in black corresponds to those with contributions below 10^{-6}.

$B(E2)$ and μ values are more sensitive to residual components beyond the $SD1G1I$ nucleon-pair subspace in the *SDGI* space than calculated energy levels. This is different from the case of semimagic and open-shell spherical nuclei, where "pair states" with squared overlaps of ∼0.64 reproduce excitation energies and $B(E2)$ results with good accuracy [41].

To study how sensitive the excitation energies are to overlaps, we perform the NPA calculation in a series of model subspaces spanned by the basis states in the *SDGI*-pair configurations. These model spaces are truncated in sequence of the basis states $|\sigma_k J_k\rangle$ with the number $N_{\rm ps}$ that $1 \leqslant k \leqslant N_{\rm ps}$. Figure 10 plots calculated energies of 2_1^+, 4_1^+, and 6_1^+ states in these truncated spaces and the corresponding squared overlaps between wave functions calculated in truncated subspaces and those calculated in the full *SDGI*-pair space. One sees these energies and overlaps converge exponentially to the expected values (though with more rapid decreases for small $N_{\rm ps}$). This behavior might be related to the procedure in optimizing the subspaces of Sec. II; similar patterns have been discussed in a number of previous truncation schemes [38,50,51].

In Tables VI and VII, we present the calculated $B(E2)$ and μ of low-lying states in the truncated space with the limitation $N_{\rm ps} = 30$, 60, 90, and 120 for ^{146}Ba and 40, 80, 120, and 160 for ^{148}Ce. The dimensions of corresponding subspaces of 2^+,

TABLE V. Sum of squared overlaps, $\sum_{\sigma_k J_k} P^{(\alpha)}_{\eta\sigma_k J_k}$ with $\eta = \pi$ or ν and $|\sigma_k J_k\rangle$ for the *SD*-pair configurations in a few yrast states of ^{146}Ba and ^{148}Ce in the full *SDGI*-pair configuration space.

^{146}Ba	0_1^+	2_1^+	4_1^+	6_1^+
Proton	0.68	0.64	0.56	0.46
Neutron	0.65	0.61	0.54	0.47
^{148}Ce	0_1^+	2_1^+	4_1^+	6_1^+
Proton	0.78	0.72	0.64	0.51
Neutron	0.67	0.63	0.57	0.51

TABLE VI. $B(E2; I \to I-2)$ (in e^2b^2) and μ (in μ_N) values for a few yrast states of ^{146}Ba in a few truncated *SDGI* spaces, versus the number of selected nucleon-pair basis states $N_{\rm ps}$. The dimensions of selected subspaces are presented, with that of "full" correspond to the case of the full *SDGI* nucleon-pair configuration space.

State	$N_{\rm ps}$	Dim.	$B(E2)$	μ
2_1^+	30	580	0.39	1.09
	60	2222	0.45	1.10
	90	4717	0.48	1.06
	120	7815	0.48	1.02
	Full	193 052	0.49	0.94
4_1^+	30	729	0.58	2.28
	60	2926	0.65	2.30
	90	6366	0.68	2.19
	120	10 713	0.69	2.13
	Full	312 342	0.71	1.94
6_1^+	30	665	0.61	3.60
	60	2852	0.71	3.61
	90	6389	0.74	3.42
	120	10 969	0.75	3.36
	Full	382 247	0.77	3.02

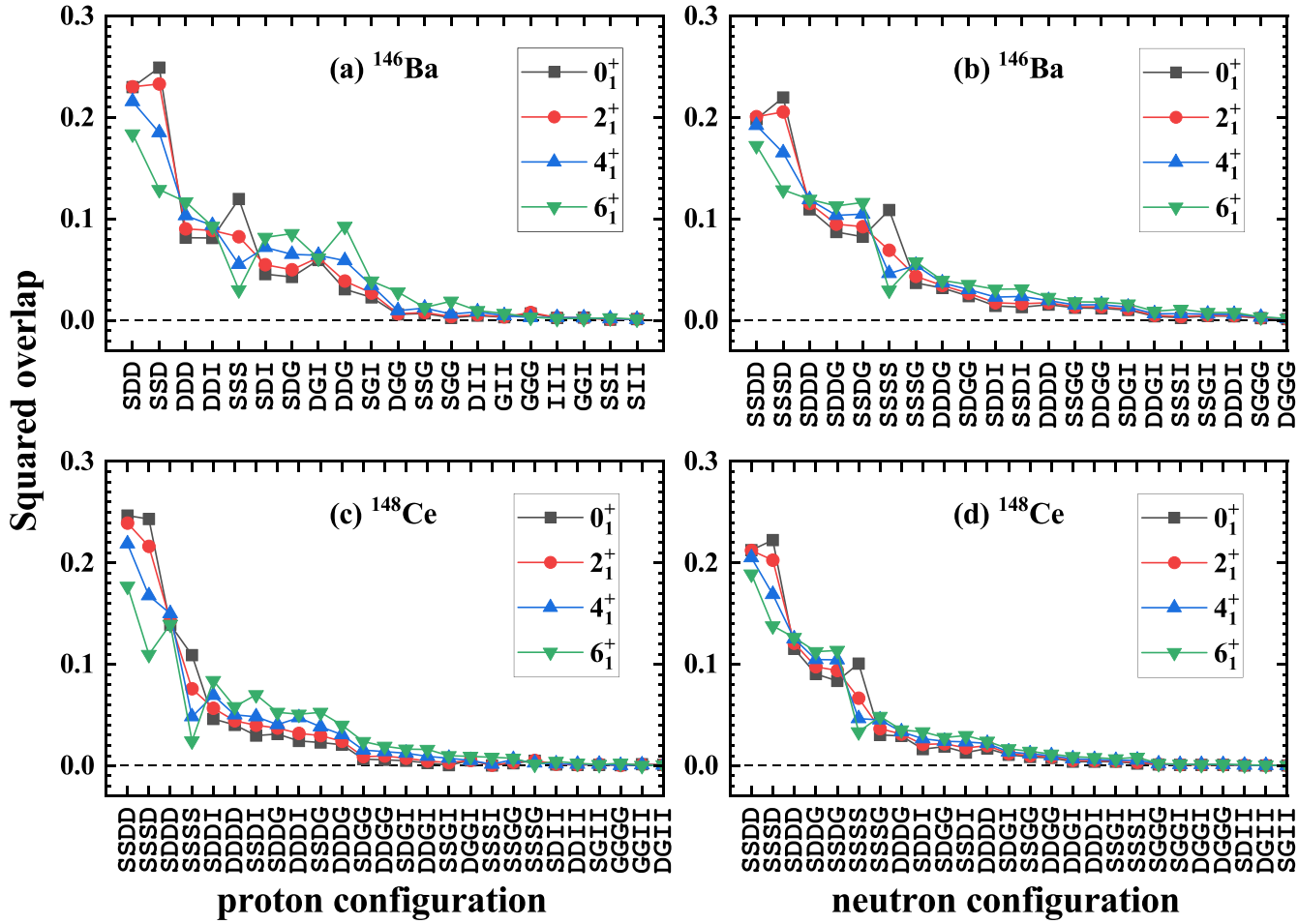

FIG. 9. Squared overlap of each specific nucleon-pair configuration with the wave function obtained in the full *SDGI*-pair space for the 0_1^+, 2_1^+, 4_1^+, and 6_1^+ states of ^{146}Ba and ^{148}Ce. Panels (a) and (c) correspond to proton configurations, and panels (b) and (d) correspond to neutron configurations. See Sec. II B for the procedure to calculate the overlaps.

4^+, and 6^+ states in each cases are also listed for comparison. One sees that calculated $B(E2)$ values in truncated subspaces converge rapidly to the value calculated in the full *SDGI*-pair space, while the μ values do not. For ^{146}Ba, one is able to well reproduce the $B(E2)$ values at $N = 120$, with the truncated space about 3% of the full *SDGI* nucleon-pair space; while for magnetic moment the average deviation of truncated nucleon-pair subspaces is about 10% (with fluctuations). Considering the exponential convergence of the overlaps shown in Fig. 10, we conclude that the magnetic moment is a more sensitive probe to the wave functions of low-lying structure in deformed nuclei.

TABLE VII. Same as Table VI but for ^{148}Ce.

State	N_{ps}	Dim.	$B(E2)$	μ
2_1^+	40	994	0.42	0.79
	80	3881	0.47	0.84
	120	8560	0.49	0.83
	160	14 453	0.50	0.82
	Full	1 089 688	0.50	0.81
4_1^+	40	1261	0.61	1.66
	80	5157	0.68	1.75
	120	11 574	0.70	1.74
	160	19 761	0.71	1.71
	Full	1 774 997	0.72	1.67
6_1^+	40	1156	0.65	2.69
	80	5104	0.73	2.75
	120	11 743	0.76	2.74
	160	202 30	0.77	2.71
	Full	2 192 601	0.78	2.59

V. SUMMARY AND DISCUSSION

To summarize, in this paper we study the nucleon-pair approximation for deformed nuclei. Explicitly, we study the contributions of different nucleon-pair basis states, with a focus on the analysis of the roles played by G and I nucleon pairs, in very large nucleon-pair configuration spaces. We demonstrate that for low-lying states of deformed nuclei, *SD* components are more predominant than previously assumed. On the one hand, G and I pairs are not negligible, and, on the other hand, with very small mixings of those configurations with the conventional *SD* nucleon-pair space, one is able to achieve reasonable agreement with exact results.

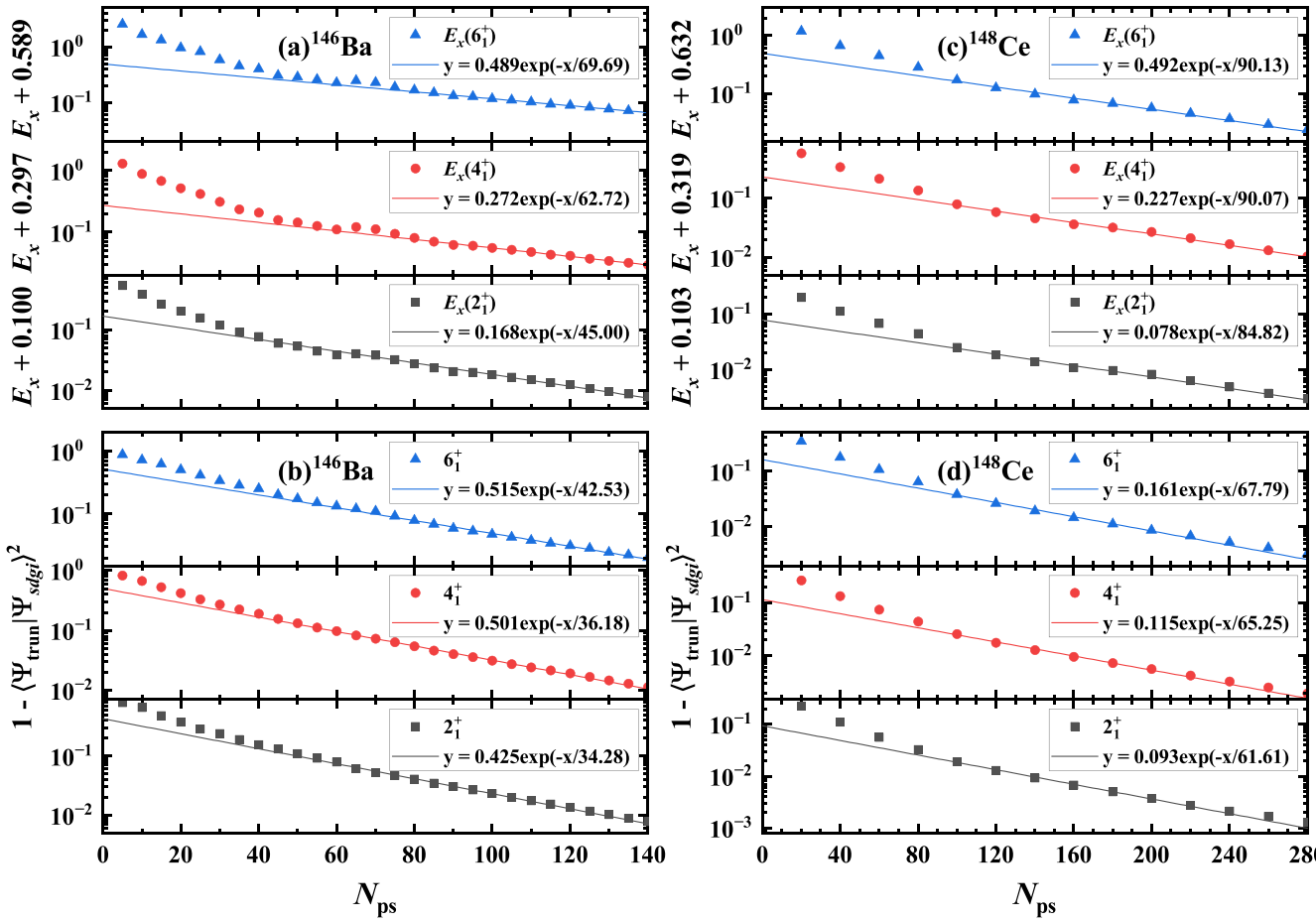

FIG. 10. Convergence of calculated excitation energies of ^{146}Ba and ^{148}Ce in truncated *SDGI* subspaces versus the number of selected, optimized nucleon-pair basis states N_{ps} (see Sec. II B for details of the procedure to optimize the basis states). Panels (a) and (c) correspond to excitation energies (in units of MeV) of a few yrast states, and panels (b) and (d) present corresponding squared overlaps between the eigenstates in the truncated spaces and those in the full *SDGI*-pair space. The solid lines are exponential curves to fit data.

In this paper, two typical forms of Hamiltonian, the Elliott's SU(3) Hamiltonian and the effective $V_{\text{low}-k}$ Hamiltonian, are investigated in a number of nucleon-pair model spaces. Both our nucleon pairs and corresponding structure coefficients are derived from the Hartree-Fock ground states, which was used in Ref. [27] and exemplified in Ref. [28] for deformed nuclei. In the first case, the excitation energies E_x and reduced electric quadrupole transition probabilities $B(E2)$ of systems, with six valence protons and six valence neutrons or with eight valence protons and eight valence neutrons, in the *pf* shell in the presence of the SU(3) quadrupole-quadrupole interaction, calculated in the full *SDGI* nucleon-pair configuration space, are in excellent agreement with the exact values from analytic solutions of the Elliott model. In the second case we calculate E_x and $B(E2)$ values of ^{146}Ba and ^{148}Ce in the presence of $V_{\text{low}-k}$ effective interaction in both the full and a number of truncated *SDGI* nucleon-pair configuration spaces.

Among the calculated results in these truncated nucleon-pair configuration spaces, we obtain good agreement and quick convergence for energy levels. As is well known, calculated $B(E2)$ and magnetic moments are seen to be more sensitive to the configuration space beyond the so-called *SD*1*G*1*I* configuration space than calculated energy levels. As expected, for the SU(3) model we need the configurations including two *I* pairs in order to satisfactorily reproduce the $B(E2)$ values from the *SDGI* approximation; for realistic nuclei, ^{146}Ba and ^{148}Ce, some configurations with two *G* pairs are useful to reproduce the moments of inertia in the *SDGI* approximation.

This study provides us with a simple pattern for the components of the low-lying states in the deformed nuclei. First, the distribution of wave function in terms of nucleon-pair configurations is very similar for different states in the yrast band, and, second, the *SD*-pair configurations contribute the most important proportion in the low-lying states by usually over 50%. The configurations with only one *G* and/or *I* pair(s) contribute the second important, and all other configurations are much less important, as a whole. This study lay foundation and benchmark of simplifications in the NPA studies of low-lying states for deformed nuclei in future.

In order to study how compact a subspace could be under the requirement of reasonable accuracy in description of physical observables, we perform the NPA calculation in a number

of model spaces constructed by nucleon-pair basis states. We find that it is relatively easier to obtain convergence for calculated energy levels, next for $B(E2)$ values, and relatively more difficult to obtain convergence for calculated magnetic moments, as we expand the subspaces step by step in the full *SDGI* subspace. This means that, at least for these deformed nuclei, the magnetic moment is a much more sensitive probe to the nuclear wave function, comparing to the excitation energy and $B(E2)$.

ACKNOWLEDGMENTS

One of the authors (C. Ma) is grateful to Professor G. J. Fu for discussions. We thank the National Natural Science Foundation of China (Grants No. 12375114, No. 11975151, and No. 11961141003), the Joint Research Program with the HIRFL-CSR mass measurement in the Institute of Modern Physics, CAS, and the MOE Key Lab for Particle Physics, Astrophysics and Cosmology, for financial support.

[1] M. G. Mayer, Phys. Rev. **75**, 1969 (1949).
[2] J. H. D. Jensen, H. E. Sueß, and O. Haxel, Naturwissenschaften **36**, 155 (1949).
[3] R. Machleidt, Phys. Rev. C **63**, 024001 (2001).
[4] B. A. Brown and B. H. Wildenthal, Annu. Rev. Nucl. Part. Sci. **38**, 29 (1988); B. A. Brown and W. A. Richter, Phys. Rev. C **74**, 034315 (2006); A. Magilligan and B. A. Brown, *ibid.* **101**, 064312 (2020).
[5] M. Honma, B. A. Brown, T. Mizusaki, and T. Otsuka, Nucl. Phys. A **704**, 134 (2002); M. Honma, T. Otsuka, B. A. Brown, and T. Mizusaki, Phys. Rev. C **65**, 061301(R) (2002); Eur. Phys. J. A **25**, 499 (2005).
[6] A. Poves, J. Sánchez-Solano, E. Caurier, and F. Nowacki, Nucl. Phys. A **694**, 157 (2001).
[7] C. Qi and F. R. Xu, Nucl. Phys. A **800**, 47 (2008).
[8] M. Honma, T. Otsuka, T. Mizusaki, and M. Hjorth-Jensen, Phys. Rev. C **80**, 064323 (2009).
[9] E. Caurier, G. Martínez-Pinedo, F. Nowack, A. Poves, and A. P. Zuker, Rev. Mod. Phys. **77**, 427 (2005).
[10] T. Otsuka, Y. Tsunoda, T. Abe, N. Shimizu, and P. Van Duppen, Phys. Rev. Lett. **123**, 222502 (2019); Y. Tsunoda and T. Otsuka, Configuration interaction approach to atomic nuclei: The shell model, in *Handbook of Nuclear Physics* (Springer, Singapore, 2023), pp. 2179–2227.
[11] M. L. Liu, and C. X. Yuan, Int. J. Mod. Phys. E **32**, 2330003 (2023).
[12] G. Racah, Phys. Rev. **62**, 438 (1942); **63**, 367 (1943).
[13] I. Talmi, *Simple Models of Complex Nuclei* (Harwood Academic, Chur, 1993).
[14] I. Talmi, Nucl. Phys. A **172**, 1 (1971).
[15] S. Shlomo and I. Talmi, Nucl. Phys. A **198**, 81 (1972).
[16] F. Q. Luo and M. A. Caprio, Nucl. Phys. A **849**, 35 (2011).
[17] K. Allart, E. Boeker, G. Bonsignori *et al.*, Phys. Rep. **169**, 209 (1988); Y. K. Gambir, S. Haq, and J. K. Suri, Ann. Phys. (NY) **133**, 154 (1981).
[18] C. L. Wu, Da Hsuan Feng, X. G. Chen, J. Q. Chen, and M. W. Guidry, Phys. Rev. C **36**, 1157 (1987); C. L. Wu, D. F. Feng, and M. Guidry, in *Advances in Nuclear Physics*, edited by J. W. Negele and E. W. Vogt (Preenum Press, New York, 1994), pp. 227–443.
[19] J. Q. Chen, Nucl. Phys. A **626**, 686 (1997); Y. M. Zhao, N. Yoshinaga, S. Yamaji, J. Q. Chen, and A. Arima, Phys. Rev. C **62**, 014304 (2000); Y. M. Zhao and A. Arima, Phys. Rep. **545**, 1 (2014).
[20] A. Arima and F. Iachello, Phys. Rev. Lett. **35**, 1069 (1975); Ann. Phys. **99**, 253 (1976); **111**, 201 (1978); **123**, 468 (1979).
[21] T. Otsuka, A. Arima, F. Iachello, and I. Talmi, Phys. Lett. B **76**, 139 (1978).
[22] J. N. Ginocchio and C. W. Johnson, Phys. Rep. **264**, 153 (1996).
[23] N. Yoshinaga, T. Mizusaki, A. Arima, and Y. D. Devi, Prog. Theor. Phys. Suppl. **125**, 65 (1996).
[24] Y. M. Zhao, S. Yamaji, N. Yoshinaga, and A. Arima, Phys. Rev. C **62**, 014315 (2000); H. Jiang, Y. Lei, C. Qi, R. Liotta, R. Wyss, and Y. M. Zhao, *ibid.* **89**, 014320 (2014).
[25] A. Bohr and B. R. Mottelson, Phys. Scr. **22**, 468 (1980); **25**, 915 (1982); T. Otsuka, A. Arima, and N. Yoshinaga, Phys. Rev. Lett. **48**, 387 (1982).
[26] N. Yoshinaga, Nucl. Phys. A **503**, 65 (1989).
[27] G. J. Fu and C. W. Johnson, Phys. Lett. B **809**, 135705 (2020).
[28] G. J. Fu and C. W. Johnson, Phys. Rev. C **104**, 024312 (2021).
[29] J. P. Elliott, Proc. R. Soc. Lond. A **245**, 128 (1958); **245**, 562 (1958).
[30] G. J. Fu, Y. Lei, Y. M. Zhao, S. Pittel, and A. Arima, Phys. Rev. C **87**, 044310 (2013).
[31] Y. Y. Cheng, Y. M. Zhao, and A. Arima, Phys. Rev. C **97**, 024303 (2018).
[32] B. C. He, L. Li, Y. A. Luo, Y. Zhang, F. Pan, and J. P. Draayer, Phys. Rev. C **102**, 024304 (2020); Y. Lei, Y. Lu, and Y. M. Zhao, Chin. Phys. C **45**, 054103 (2021).
[33] C. Ma, X. Yin, and Y. M. Zhao, Phys. Rev. C **108**, 034308 (2023).
[34] I. Stetcu and C. W. Johnson, Phys. Rev. C **66**, 034301 (2002).
[35] G. J. Fu, Calvin W. Johnson, P. Van Isacker, and Z. Ren, Phys. Rev. C **103**, L021302 (2021).
[36] F. Iachello and I. Talmi, Rev. Mod. Phys. **59**, 339 (1987).
[37] P. Halse, Phys. Rev. C **39**, 1104 (1989).
[38] T. Papenbrock and D. J. Dean, Phys. Rev. C **67**, 051303(R) (2003); T. Papenbrock, A. Juodagalvis, and D. J. Dean, *ibid.* **69**, 024312 (2004).
[39] Z. Y. Xu, Y. Lei, Y. M. Zhao, S. W. Xu, Y. X. Xie, and A. Arima, Phys. Rev. C **79**, 054315 (2009).
[40] C. Qi, J. Blomqvist, T. Bäck, B. Cederwall, A. Johnson, R. J. Liotta, and R. Wyss, Phys. Rev. C **84**, 021301(R) (2011).
[41] Y. Y. Cheng, Y. M. Zhao, and A. Arima, Phys. Rev. C **94**, 024307 (2016); Y. Y. Cheng, C. Qi, Y. M. Zhao, and A. Arima, *ibid.* **94**, 024321 (2016); Y. Y. Cheng, H. Wang, J. J. Shen, X. R. Zhou, Y. M. Zhao, and A. Arima, *ibid.* **100**, 024321 (2019).
[42] M. Harvey, The nuclear SU_3 model, in *Advances in Nuclear Physics* (Springer, Boston, MA, 1968).
[43] K. V. K. Brahmam, R. D. R. Raju, and R. Raju, At. Data Nucl. Data Tables **16**, 165 (1975).
[44] Y. M. Zhao, N. Yoshinaga, S. Yamaji, and A. Arima, Phys. Rev. C **62**, 014316 (2000).
[45] M. S. Fayache, Y. Y. Sharon, and L. Zamick, Phys. Rev. C **55**, 1575 (1997); E. Moya de Guerra, P. Sarriguren, and L. Zamick, *ibid.* **56**, 863 (1997).

[46] National Nuclear Data Center, https://www.nndc.bnl.gov/.
[47] S. Bogner, T. T. S. Kuo, L. Coraggio, A. Covello, and N. Itaco, Phys. Rev. C **65**, 051301(R) (2002).
[48] S. K. Bognera, T. T. S. Kuo, and A. Schwenk, Phys. Rep. **386**, 1 (2003).
[49] N. Yoshinaga, Nucl. Phys. A **570**, 421 (1994).
[50] N. Yoshinaga and A. Arima, Phys. Rev. C **81**, 044316 (2010).
[51] J. J. Shen, Y. M. Zhao, and A. Arima, Phys. Rev. C **82**, 014309 (2010); **85**, 064325 (2012); J. J. Shen, Y. M. Zhao, A. Arima, and N. Yoshinaga, *ibid.* **83**, 044322 (2011).